# Multimeric Anti-DR5 IgM Agonist Antibody IGM-8444 Is a Potent Inducer of Cancer Cell Apoptosis and Synergizes with Chemotherapy and BCL-2 Inhibitor ABT-199

Beatrice T. Wang, Tasnim Kothambawala, Ling Wang, Thomas J. Matthew, Susan E. Calhoun, Avneesh K. Saini, Maya F. Kotturi, Genevive Hernandez, Eric W. Humke, Marvin S. Peterson, Angus M. Sinclair, and Bruce A. Keyt

## ABSTRACT

Death receptor 5 (DR5) is an attractive target for cancer therapy due to its broad upregulated expression in multiple cancers and ability to directly induce apoptosis. Though anti-DR5 IgG antibodies have been evaluated in clinical trials, limited efficacy has been attributed to insufficient receptor crosslinking. IGM-8444 is an engineered, multivalent agonistic IgM antibody with 10 binding sites to DR5 that induces cancer cell apoptosis through efficient DR5 multimerization. IGM-8444 bound to DR5 with high avidity and was substantially more potent than an IgG with the same binding domains. IGM-8444 induced cytotoxicity in a broad panel of solid and hematologic cancer cell lines but did not kill primary human hepatocytes *in vitro*, a potential toxicity of DR5 agonists. In multiple xenograft tumor models, IGM-8444 monotherapy inhibited tumor growth, with strong and sustained tumor regression observed in a gastric PDX model. When combined with chemotherapy or the BCL-2 inhibitor ABT-199, IGM-8444 exhibited synergistic *in vitro* tumor cytotoxicity and enhanced *in vivo* efficacy, without augmenting *in vitro* hepatotoxicity. These results support the clinical development of IGM-8444 in solid and hematologic malignancies as a monotherapy and in combination with chemotherapy or BCL-2 inhibition.

## Introduction

Death receptor 5 (DR5, TNFRSF10B) is a member of the TNF receptor superfamily that binds TNF-related apoptosis inducing ligand (TRAIL, TNFSF10), and activates the extrinsic apoptotic pathway upon receptor multimerization. DR5 clustering enables formation of the death-inducing signaling complex (DISC) through Fas-associated death domain recruitment to the DR5 intracellular death domain, subsequent recruitment and cleavage of procaspase-8 and -10, and downstream activation of effector caspase-3 and -7 (1). DR5 is homologous to TRAIL-binding apoptotic death receptor 4 (DR4, TNFRSF10A) and two decoy receptors, DcR1 (TNFRSF10C) and DcR2 (TNFRSF10D) that lack or have a truncated death domain.

DR5 is a promising cancer therapeutic target more highly expressed on cancer cells than normal human tissues, providing selective tumor killing (2, 3). Recombinant TRAIL and anti-DR5 agonistic IgG antibodies have demonstrated efficacy in preclinical mouse tumor models (4–9) and were safe in cynomolgus monkeys (10, 11). Although these agents were generally well tolerated in patients, there were select reports of on-target, off-tumor drug-induced hepatotoxicity (12, 13). These first-generation DR5 agonists failed to demonstrate significant clinical efficacy, alone or combined with chemotherapy (reviewed in ref. 14). For recombinant TRAIL, this was largely attributed to its very short half-life (<1 hour in humans, ref. 15) and ability to bind the non-apoptotic signaling decoy receptors. Although the anti-DR5 agonistic IgG antibodies had good pharmacokinetic properties, the lack of efficacy was attributed to insufficient DR5 receptor clustering and suboptimal FcγR-mediated receptor crosslinking (1). Recent structural data suggest that formation of higher order DR5 clusters, including dimers of trimers, is required for efficient DR5 signaling (16).

To mitigate the need for FcγR-mediated receptor crosslinking, we have taken the approach to multimerize and agonize DR5 using an immunoglobulin M (IgM) antibody format. With strong antigen-binding avidity, IgM is particularly effective at binding repetitive epitopes and low expressing antigens. We hypothesized that a multivalent IgM should effectively cluster and agonize TNF receptor superfamily members, including DR5. We and others have previously demonstrated that IgM antibodies targeting DR5 and DR4 exhibit functional activity in the absence of crosslinking (17–21). Here, we describe the development of our clinical candidate IGM-8444, a novel pentameric DR5-targeting IgM antibody, which was substantially more potent than a corresponding agonistic DR5 IgG and induced apoptosis across multiple solid and hematological cancer types *in vitro*. Despite its cytotoxic activity on cancer cell lines, IGM-8444 did not kill primary human hepatocytes *in vitro*. IGM-8444 exhibited efficacy in both cell line and patient-derived xenograft (PDX) mouse tumor models, accompanied by increased apoptotic biomarkers in circulation and tumor tissue. Combinations of IGM-8444 with standard-of-care (SOC) chemotherapy or targeted agents induced synergistic *in vitro* tumor cytotoxicity and enhanced *in vivo* efficacy relative to those therapies alone. Taken together, these data support that multimerizing DR5 with IGM-8444 is a promising therapeutic approach for cancer therapy.

IGM Biosciences Inc., Mountain View, California.

**Note:** Supplementary data for this article are available at Molecular Cancer Therapeutics Online (http://mct.aacrjournals.org/).

T. Kothambawala, L. Wang, and T.J. Matthew contributed equally as co-authors of this article.

**Corresponding Author:** Bruce A. Keyt, IGM Biosciences Inc., 325 East Middlefield Road, Mountain View, CA 94043. Phone: 650-965-7873; Fax: 650-426-0566; E-mail: bkeyt@igmbio.com

Mol Cancer Ther 2021;XX:XX–XX

**doi:** 10.1158/1535-7163.MCT-20-1132

## Materials and Methods

### Antibody generation

The IGM-8444 VH and VL sequences are shown in Supplementary Table S1A. The DR5-binding VH domains were cloned into an IgM or IgG1 backbone and transfected into Chinese hamster ovary (CHO) cells with the DR5-binding light chain, as well as the joining (J) chain for IgMs. IgG and IgM antibodies were purified using Protein A affinity chromatography (GE Healthcare Life Sciences) and published methods (22), respectively. IGM-8444 characterization by SDS-PAGE, size exclusion chromatography (SEC)-HPLC, and dynamic light scattering (DLS) is described in Supplementary Methods.

### Cell lines and reagents

Colo205 and MV-411 cells were obtained from the ATCC, H-EMC-SS cells from ECACC, HCT15 and NCI-H2228 cells from Crown Bioscience. Cells were cultured according to the source recommendations, authenticated by STR profiling and confirmed negative for *Mycoplasma* by PCR (IDEXX Bioanalytics). For screening, cell lines were provided and cultured as per Crown Bioscience protocols. Human IgG and IgM isotype controls were from Jackson ImmunoResearch. Chemotherapeutic agents and BCL-2 inhibitor ABT-199 were from MedChemExpress and Selleck Chemicals. For animal studies, irinotecan and 5-FU were obtained from Fresenius Kabi, paclitaxel from Phyton Biotech, and ABT-199 from Selleck.

### Binding assays

Antibody affinity and avidity were measured using surface plasmon resonance (SPR) and DR5 specificity by ELISA (Supplementary Methods). Colo205 and H-EMC-SS (50,000 cells/well) were incubated with IGM-8444 or anti-DR5 IgG for 35 minutes at 4°C. IgG and IgM isotype controls were used at 10 μg/mL. Cells were washed with FACS stain buffer (BD Biosciences), incubated with 1 μg/mL of goat anti-human kappa-Alexa Fluor 647 (Southern Biotech #2060–31) for 30 minutes at 4°C, washed, resuspended with 100 μL/well of 7-AAD (BD Biosciences) diluted in FACS stain buffer and analyzed using a Beckman Coulter CytoFLEX flow cytometer.

### Cytotoxicity assays

Colo205 and H-EMC-SS (3,000 cells/well) were seeded in half-area 96-well plates, incubated overnight at 37°C, then treated with IGM-8444 or anti-DR5 IgG for 24 hours at 37°C. For combination studies, HCT-15 (2,000 cells/well) and NCI-H2228 (8,000 cells/well) were seeded in 96-well plates, incubated overnight, and treated with IGM-8444 and chemotherapy or ABT-199 for 72 hours. MV-411 (3,000 cells/well) were seeded in half-area 96-well plates and treated with combined therapy as above. Cell viability was measured using CellTiter-Glo (Promega) and read on an EnVision luminometer (PerkinElmer). $IC_{50}$ values were calculated in GraphPad Prism using a 4-parameter curve fit.

Primary human hepatocytes from mixed gender, 10-donor pools (BioIVT) were plated in INVITROGRO CP media supplemented with 1x Torpedo antibiotic mix (BioIVT). Hepatocytes (56,000 cells/well) were seeded in 96-well collagen-coated plates and incubated at 37°C overnight, then treated with IGM-8444 or recombinant human TRAIL ligand (R&D Systems #375-TL-010/CF) for 24 hours. For combination studies, IGM-8444 and chemotherapeutic agents or ABT-199 were incubated for 72 hours. Cell viability was measured as described above.

### Apoptosis assays

3,000 cells/well were seeded in half-area 96-well plates, incubated overnight at 37°C, then treated with 1 μg/mL antibody for indicated times. At endpoint, Caspase-Glo 3/7, Caspase-Glo 8 plus MG-132 inhibitor, or Caspase-Glo 9 plus MG-132 inhibitor (Promega) was added then read on an EnVision luminometer.

Annexin V/propidium iodide (PI) staining was measured by flow cytometry. 3000 cells/well were treated with 1 μg/mL antibody as indicated. Cells were washed with DPBS, resuspended in binding buffer containing Annexin V-APC and PI (BD Biosciences), incubated for 15 minutes at 25°C protected from light, and analyzed using a CytoFLEX flow cytometer.

### *In vitro* cytotoxicity assay transformation and expression analysis

Luminescence data were processed with GRcalculator (23) to fit growth-rate-normalized dose–response curves. Secondary measurements were calculated from the GR curve to assess IGM-8444 sensitivity and efficacy ($GR_{AOC}$ and $GR_{max}$, respectively). Samples were clustered into high, medium, and low responders based on these features, and correlated with DR5 expression data (RPKM) from the CCLE (Broad Institute). A Welch's *t* test was performed between the high and low response groups to assess differences in average DR5 expression. For details, see Supplementary Methods.

### Synergy evaluation

Synergy for each cell line was computed with viability data from IGM-8444 and chemotherapy combinations analyzed for Bliss Independence (24, 25). Synergy scores were calculated and visualized in 3D surface plots with valleys of antagonism (Bliss <0) and hills of synergy (Bliss >0) over the continuum of dose combinations. For details, see Supplementary Methods.

### *In vivo* tumor xenograft models

All animal studies were conducted according to approved Institutional Animal Care and Use Committee (IACUC) protocols at Charles River Laboratories (CRL). Colo205 and NCI-H2122 models were performed in female athymic nude mice [Crl:NU (Ncr)-*Foxn1*$^{nu}$, 8–12-weeks-old; CRL]. Colo205 ($2 \times 10^6$ cells) or NCI-H2122 ($10^7$ cells) in 50% Matrigel were implanted subcutaneously in the flank and dosing initiated when mean tumor volume (MTV) reached 100–150 $mm^3$ or 80–120 $mm^3$, respectively. DOHH-2 ($10^7$ cells) were implanted subcutaneously in the flanks of female SCID mice (Fox Chase SCID, CB17/Icr-*Prkdc*$^{scid}$/IcrIcoCrl, 9-weeks-old; CRL) and dosing initiated when MTV reached 100–150 $mm^3$.

GXF251 PDX tumor fragments 3–4 mm in diameter were implanted subcutaneously in the flanks of female NMRI nude mice (5–7-weeks-old; CRL, Germany). Treatment began when MTV reached 50–250 $mm^3$. In studies evaluating larger tumors, dosing initiated when MTV reached approximately 100, 300, or 500 $mm^3$.

Tumor volume was determined by caliper measurement and tumor growth inhibition (TGI) and relative tumor volume calculations are described in Supplementary Methods. Mice were euthanized when individual tumor volumes exceeded 1,000 $mm^3$ for Colo205, 1,500 $mm^3$ for NCI-H2122, or 2,000 $mm^3$ for the DOHH-2 and GXF251 models. Tumor volume results are shown as mean ± SEM with 8–10 animals per group. A partial response (PR) was achieved if tumor volume was 50% or less than the starting tumor volume for 3 consecutive measurements. A complete response (CR) was achieved if tumor volume was undetectable for 3 consecutive measurements. Animals with a CR at study end were classified as tumor-free survivors

(TFS). For survival analyses, an event was defined as a tumor volume 4 times that of the initial volume.

### IHC

NCI-H2122 tumors were implanted as described above and dosing was initiated when MTV reached 200–250 $mm^3$. Tumors were extracted 24 hours later, fixed with 10% neutral buffered formalin for 48 hours, transferred to 70% ethanol, and paraffin embedded. IHC staining was performed using protocols and reagents from Biocare Medical using an intelliPATH FLX instrument. Sections were cut and deparaffinized, then blocked. For cleaved caspase-3 (CC3) staining, CC3 (Asp175) antibody (0.2 μg/mL, Cell Signaling Technology #9661) was diluted in Da Vinci Green diluent and incubated for 30 minutes at 25°C. After washing with TBS, slides were incubated with MACH2 Rabbit HRP-Polymer for 30 minutes. Slides were washed and developed with intelliPATH FLX DAB Chromogen for 5 minutes, rinsed with distilled water, and lightly counterstained with hematoxylin for 20 seconds. For DR5 staining, tumor sections were stained for human DR5 (1 μg/mL, LSBio #LS-C340229) followed by detection with MACH2 Mouse HRP-Polymer, then processed as described above.

### M30 and M65 ELISA

Caspase-cleaved cytokeratin 18 (CK18-Asp396) exposed during apoptosis in mouse sera was quantitated by M30-Apoptosense ELISA, and total CK18 was quantitated by M65 ELISA (PEVIVA) according to the manufacturer's protocol. Plates were read on a Spectra Max340 microplate reader using SoftMax Pro V5 (Molecular Devices).

### Statistical analysis

TGI was calculated on the last day that all control animals were on study. Mann–Whitney U tests were used for pairwise tumor volume comparisons between treated versus control groups. Kruskal–Wallis analysis with Dunn's post-test was used to compare tumor volumes across multiple treatment groups. Log-rank (Mantel–Cox) tests were used to compare Kaplan–Meier survival curves. For multiple comparisons, log-rank test $P$ values were adjusted using Bonferroni–Holm correction. Statistical analyses were performed using GraphPad Prism software. A two-tailed value of $P \leq 0.05$ was considered statistically significant.

## Results

### Multivalent IGM-8444 binds strongly and specifically to DR5

IGM-8444 has 10 DR5-binding sites and assembles into a pentamer through a J chain. CHO-expressed IGM-8444 (~900 kDa) yielded a homogeneous population with >95% purity and hydrodynamic radius of 13.9 nm as determined by SDS-PAGE, SEC, and DLS (Supplementary Fig. S1A–S1D). The affinity and avidity of multivalent IGM-8444 versus bivalent anti-DR5 IgG (with same binding domains) were measured using SPR. At low DR5 densities, IGM-8444 and anti-DR5 IgG had similar monovalent binding affinities (85 and 107 nmol/L, respectively). However, at higher densities of DR5, IGM-8444 had slower dissociation kinetics with an apparent avidity of <11 pmol/L compared with 7 nmol/L for anti-DR5 IgG, supporting higher IGM-8444 DR5–binding avidity (Supplementary Fig. S1E). Furthermore, in Octet binding studies, IGM-8444 out-competed anti-DR5 IgG for receptor binding, with 17 nmol/L of IGM-8444 almost completely blocking binding of 67 nmol/L anti-DR5 IgG (Supplementary Fig. S1F).

In specificity analyses, IGM-8444 bound to human DR5, but not to related receptors DR4, DcR1, or DcR2 (58%, 52%, and 56% identity, respectively; Supplementary Fig. S2A; refs. 26–28). IGM-8444 also did not bind to HEK293T cells with DR5 knocked out (Supplementary Fig. S2B and S2C). Epitope mapping studies revealed that IGM-8444 binds a membrane distal domain on DR5 within cysteine-rich domain 1 (CRD1; ref. 29).

### IGM-8444 potently induces cancer cell cytotoxicity *in vitro* compared with IgG

Cell binding and cytotoxicity studies were performed to understand whether the high IGM-8444 binding avidity could multimerize DR5 to induce cancer cell apoptosis. IGM-8444 bound strongly to DR5-expressing Colo205 colorectal cells ($EC_{50}$ 170 ng/mL; 200 pmol/L) and H-EMC-SS chondrosarcoma cells ($EC_{50}$ 64 ng/mL; 73 pmol/L) compared with anti-DR5 IgG [$EC_{50}$ >10,000 ng/mL (>70 nmol/L)] on both cell lines (**Fig. 1A**). Though anti-DR5 IgG bound weakly on Colo205 and H-EMC-SS, it bound similarly to IGM-8444 on a recombinant QT6 cell line overexpressing human DR5, suggesting an IGM-8444 binding advantage on lower antigen-expressing cells (Supplementary Fig. S2D). In cytotoxicity assays, IGM-8444 was >10,000-fold more potent than anti-DR5 IgG on Colo205 cells [$IC_{50}$ 1.1 ng/mL vs. >10,000 ng/mL (1.3 pmol/L vs. >70 nmol/L), respectively] and >1,000-fold more potent on H-EMC-SS cells [$IC_{50}$ 0.32 ng/mL vs. 330 ng/mL (0.37 pmol/L vs. 2.3 nmol/L), respectively; **Fig. 1B**]. These results suggest that potent IGM-8444 cytotoxicity is achieved with <1% maximal DR5 binding on these cell lines, and similar observations have been made with other multivalent DR5 agonists (30, 31).

The mechanism of IGM-8444–mediated cell death was also investigated. Previous studies confirmed caspase-8 cleavage at the DISC, supporting the ability of IGM-8444 to induce receptor clustering (29). Caspase-3/7, caspase-8, and caspase-9 activity increased over time in IGM-8444–treated cells, reaching a maximum of 8.7-, 5.2-, and 3.5-fold, respectively, in 6 hours in Colo205 and 43-, 5.0-, and 8.7-fold, respectively, in 4–6 hours in H-EMC-SS compared with untreated cells (**Fig. 1C**). The kinetics of anti-DR5 IgG were slower and less in magnitude compared with IGM-8444. Annexin V and PI staining were used to identify early and late apoptotic cells. After 6-hour IGM-8444 treatment, 23% of Colo205 and 15% of H-EMC-SS cells were Annexin V positive, compared with only 4% and 2%, respectively, after anti-DR5 IgG treatment, similar to isotype controls (**Fig. 1D**). These data demonstrate IGM-8444 more potently and rapidly induce apoptosis compared with anti-DR5 IgG.

### IGM-8444 has a favorable *in vitro* and in *vivo* safety profile

The potential for IGM-8444 to induce hepatotoxicity was evaluated *in vitro* using primary human hepatocytes. IGM-8444 did not induce killing of pooled primary human hepatocytes at concentrations up to 500 μg/mL, more than 5 orders of magnitude higher than concentrations required to kill Colo205 cells *in vitro* (**Fig. 1E**). In comparison, recombinant TRAIL killed 58% of pooled primary human hepatocytes with an $IC_{50}$ of 0.04 μg/mL, only approximately 5-fold above concentrations required to kill Colo205 tumor cells. In cynomolgus monkeys, repeat dosing of IGM-8444 up to 30 mg/kg did not show significant elevation of serum liver enzymes compared with control animals (Supplementary Table S1B).

### IGM-8444 is potent across multiple cancer indications

IGM-8444–mediated cytotoxicity was evaluated across a panel of cell lines from 20 different cancer indications, with 177 cell lines from 15 solid tumors and 13 cell lines from 5 hematologic malignancies. Of 190 cell lines, 25 were high, 75 were moderate, and 90 were low

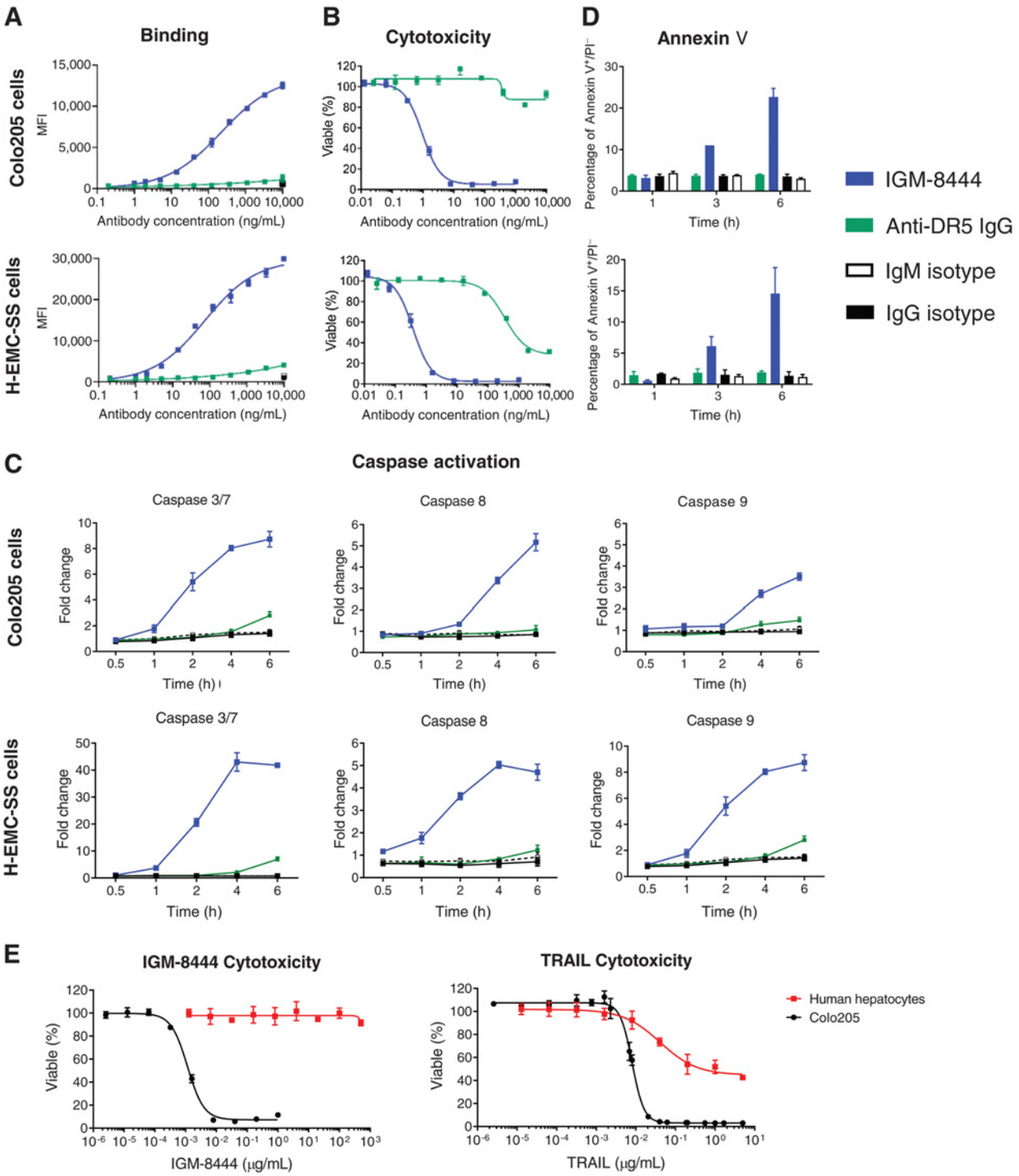


**Figure 1.**

IGM-8444 rapidly and potently induces apoptosis in Colo205 and H-EMC-SS tumor cells compared with anti-DR5 IgG while sparing hepatocytes. **A,** Cell binding was measured by flow cytometry. **B,** Cell viability was measured after 24-hour antibody treatment. **C,** Kinetics of caspase-3/7, caspase-8, and caspase-9 activation. **D,** The kinetics of apoptotic induction was determined as a percentage of Annexin V–positive and PI-negative cells by flow cytometry. **E,** Viability of primary human hepatocytes and Colo205 cells treated with IGM-8444 or recombinant TRAIL for 24 hours. A representative of two independent experiments is shown.

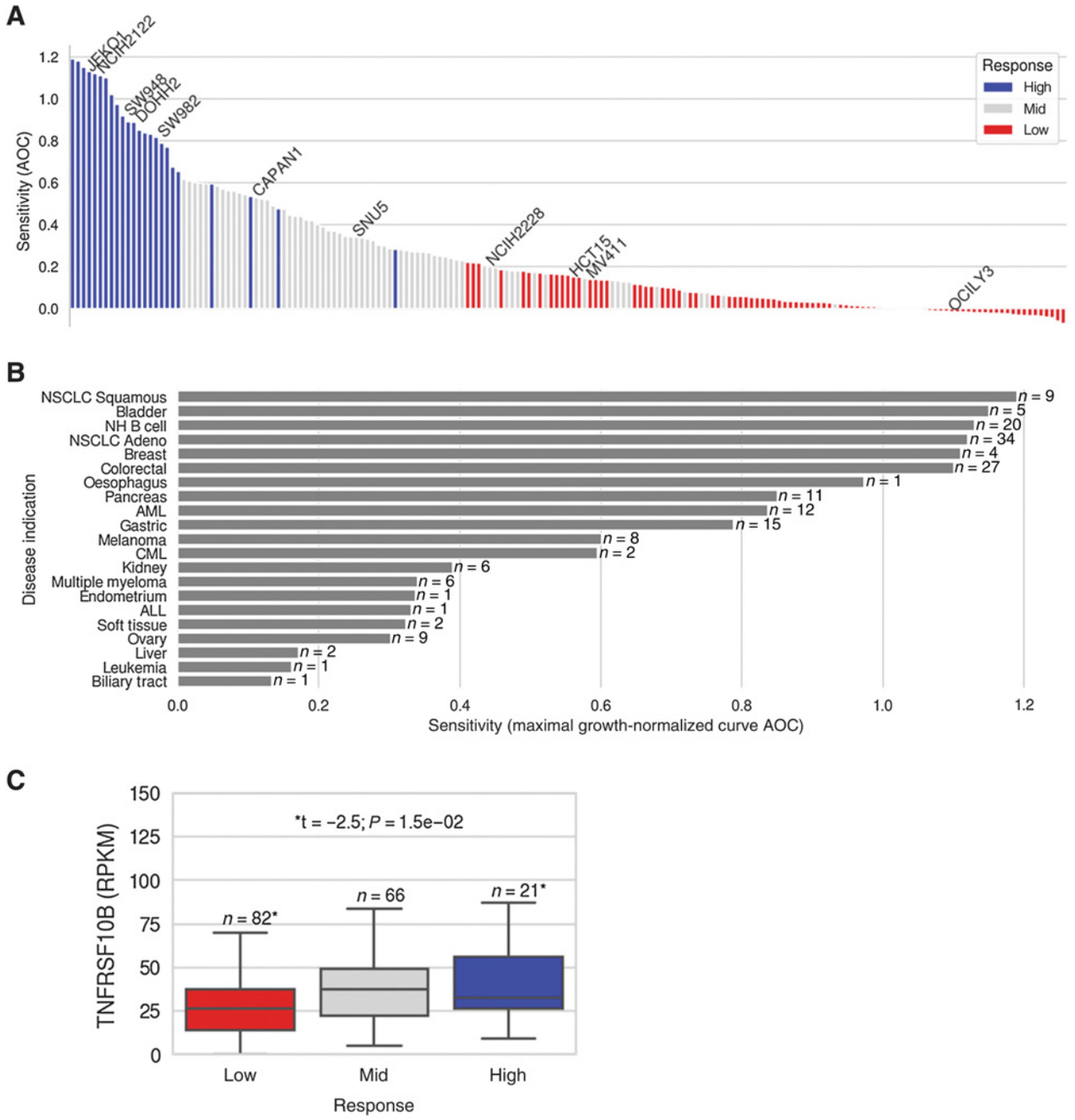


**Figure 2.**

IGM-8444 demonstrates cytotoxicity across multiple tumor lines from different cancer indications. Tumor cell lines ($n = 190$) were treated with IGM-8444 for 96 hours and viability was normalized for growth rate. **A,** Distribution of area over the curve (AOC) for the growth rate normalized dose response curve of 157 solid and 53 hematological cancer cell lines. **B,** Indications are sorted and scaled by the distribution of maximal AOC in order of sensitive to insensitive. **C,** DR5 expression associates with tiers of cytotoxic response. CCLE cell lines with a highly sensitive cytotoxic response, blue, had higher average RNA expression of DR5 compared with cell lines exhibiting low sensitivity and cytostatic growth, red ($t = 2.5$; $P = 0.015$).

responders (**Fig. 2A**; Supplementary Fig. S3). The high responder group had more potent $IC_{50}$ values (<2 ng/mL; <2 pmol/L) and greater maximal cytotoxicity ($GR_{AOC,min} > 0.28$, $GRmax_{min} > -0.87$), and included colorectal, sarcoma, lung, lymphoma, gastric and pancreatic cell lines. Maximum responses were observed in colorectal, lung, gastric and lymphoma cell lines (**Fig. 2B**). Squamous non–small cell lung cancer (NSCLC) was the most sensitive lung subtype ($GR_{AOC,max} = 1.2$, $n = 9$), with 33% having a high cytotoxic response. The high responder group had higher average DR5 RNA expression compared with low responders ($t = 2.5$, $P = 0.015$; **Fig. 2C**).

### IGM-8444 synergizes with chemotherapy and a BCL-2 inhibitor in cancer cells without hepatotoxicity

Partially sensitive cell lines were selected to evaluate IGM-8444 in combination with chemotherapeutic agents or the BCL-2 inhibitor, ABT-199. Synergy was evaluated by Bliss Independence where a Bliss score >5 indicates synergistic cytotoxicity. IGM-8444 synergized with irinotecan or oxaliplatin on HCT15 colorectal cells, with the highest average synergy in combination with irinotecan ($Bliss_{avg}$ = 13.2; **Fig. 3A**). Combination of IGM-8444 with irinotecan at maximal synergy ($Bliss_{max}$ = 30.2) showed 89.3% cytotoxicity, compared with 35.3% and 36.7% cytotoxicity for IGM-8444 and irinotecan, respectively, as single agents (Supplementary Table S2A). In NCI-H2228 NSCLC cells, IGM-8444 with paclitaxel or gemcitabine induced synergistic cytotoxicity, with highest average synergy seen with paclitaxel ($Bliss_{avg}$ = 14.7; **Fig. 3B**). IGM-8444 and paclitaxel single agents, respectively, showed 17.3% and 52.0% cytotoxicity at concentrations of maximal synergy ($Bliss_{max}$ = 25.6), whereas the combination showed 85.9% cytotoxicity (Supplementary Table S2A). In MV-411 AML cells, IGM-8444 synergized with cytarabine, doxorubicin, or ABT-199 (**Fig. 3C**), with the highest average synergy in combination with ABT-199 ($Bliss_{avg}$ = 22.5). At maximal synergy ($Bliss_{max}$ = 53.4), IGM-8444 and ABT-199 combined showed 63.1% cytotoxicity, compared with 16.5% and 0% cytotoxicity for ABT-199 and IGM-8444, respectively, as single agents (Supplementary Table S2A).

To evaluate safety, IGM-8444 was also tested in combination with each of these agents on primary human hepatocytes. Though some modest cytotoxicity was observed with chemotherapeutic agents, combination with IGM-8444 did not enhance hepatocyte toxicity (**Fig. 3D–F**).

### IGM-8444 inhibits tumor growth in cell line xenografts

Sensitive tumor cell lines, Colo205 and NCI-H2122, identified from *in vitro* assays were evaluated *in vivo*. Colo205 and NCI-H2122 tumors

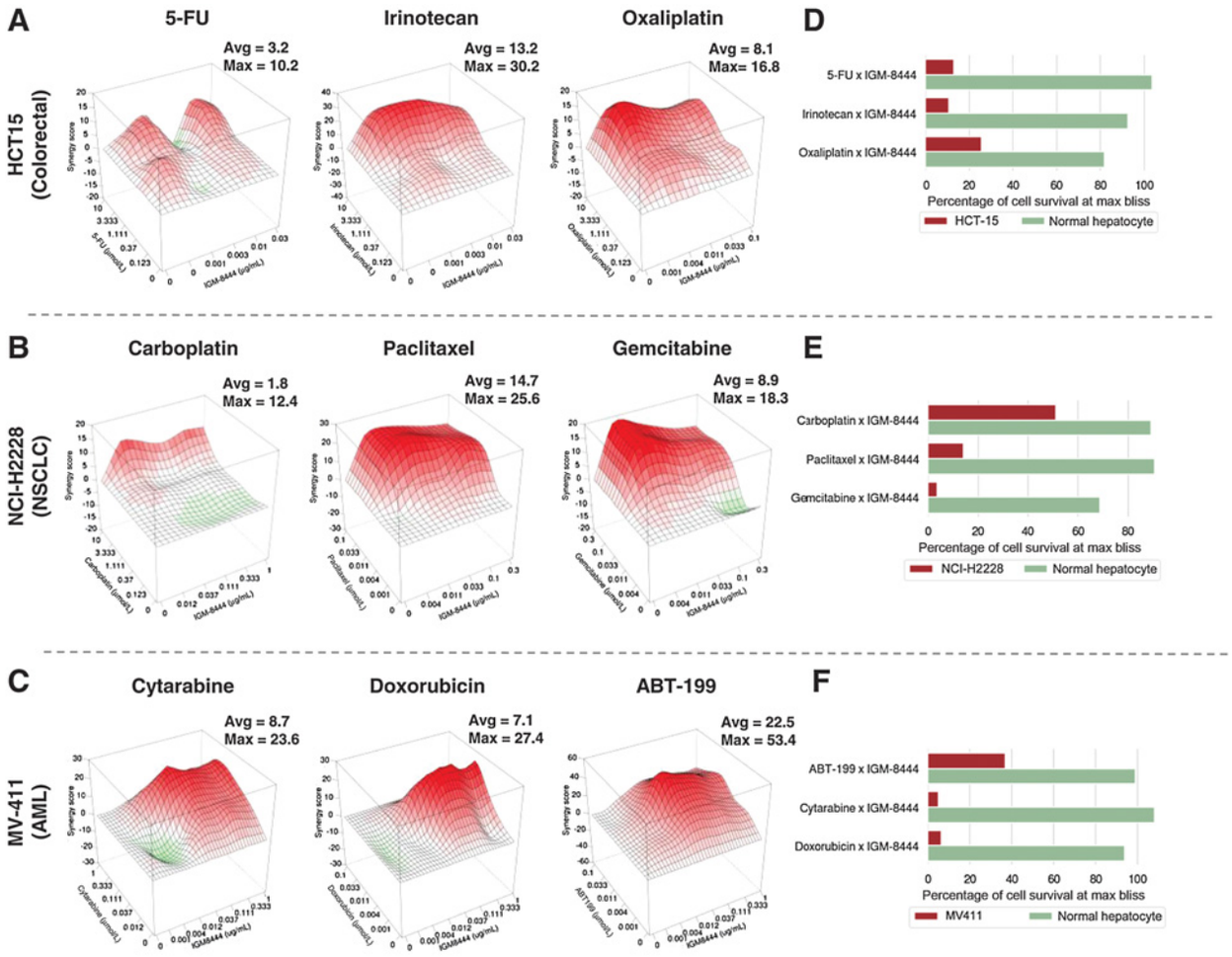


**Figure 3.**

IGM-8444 has cytotoxic synergy in combination with chemotherapeutic and targeted agents *in vitro*. HCT15 (**A**), NCI-H2228 (**B**), and MV-411 (**C**) cell lines were incubated with IGM-8444 and chemotherapy or ABT-199 alone and in combination for 72 hours, and synergy was plotted. Average and maximal Bliss scores for each combination are shown. The percentage of viable cells is shown at concentrations of maximal synergy for the HCT15 (**D**), NCI-H2228 (**E**), and MV-411 (**F**) cell lines (red), compared with viability at the corresponding concentrations when tested in normal human hepatocytes (green). Synergistic cytotoxicity was seen in cancer cell lines, whereas normal human hepatocytes generally maintained high viability even at concentrations of maximal synergy.

expressed high levels of DR5 by IHC (Supplementary Fig. S4A). In a pilot Colo205 study, a single dose of anti-DR5 IgG was administered at 3 mg/kg and IGM-8444 at 3 mg/kg daily for 5 days to approximately match serum exposure levels 24 hours after last IGM-8444 dose (Supplementary Fig. S4B). Despite 2.5-fold lower drug exposure, IGM-8444 significantly reduced tumor volumes by day 7 compared with vehicle control ($P \leq 0.01$), whereas anti-DR5 IgG did not. In subsequent studies, IGM-8444 was administered every other day to maintain serum exposures near or greater than 1 μg/mL throughout the dosing period (Supplementary Table S2B). IGM-8444 dose dependently inhibited Colo205 tumor growth during the dosing period (**Fig. 4A**). On day 22, the 0.3, 1, 3, and 10 mg/kg treatment groups exhibited 23%, 29%, 75% ($P \leq 0.01$) and 84% ($P \leq 0.001$) TGI, respectively, compared with vehicle treatment. CK18 cleavage products M30 (cleaved CK18, apoptosis biomarker) and M65 (cleaved and intact CK18, biomarker of apoptosis and necrosis) were also evaluated in serum 24 hours after the first dose. Dose-dependent increases were observed up to 10-fold with M30 and 5-fold with M65 compared with control (**Fig. 4B**).

In the NCI-H2122 xenograft model, IGM-8444 induced tumor regressions, with half the animals achieving a PR. On day 26, IGM-8444 induced 101% TGI compared with the control group ($P \leq 0.0001$; **Fig. 4C**). IGM-8444 treatment also extended median event-free survival (EFS) by 40 days ($P \leq 0.0001$; **Fig. 4D**). In NCI-H2122 pharmacodynamic studies, CC3 was significantly elevated in tumor tissue 24 hours after a single dose of IGM-8444, confirming apoptotic mechanism of action *in vivo* (**Fig. 4E**). Strong staining observed throughout each tumor indicates deep IGM-8444 tumor penetration.

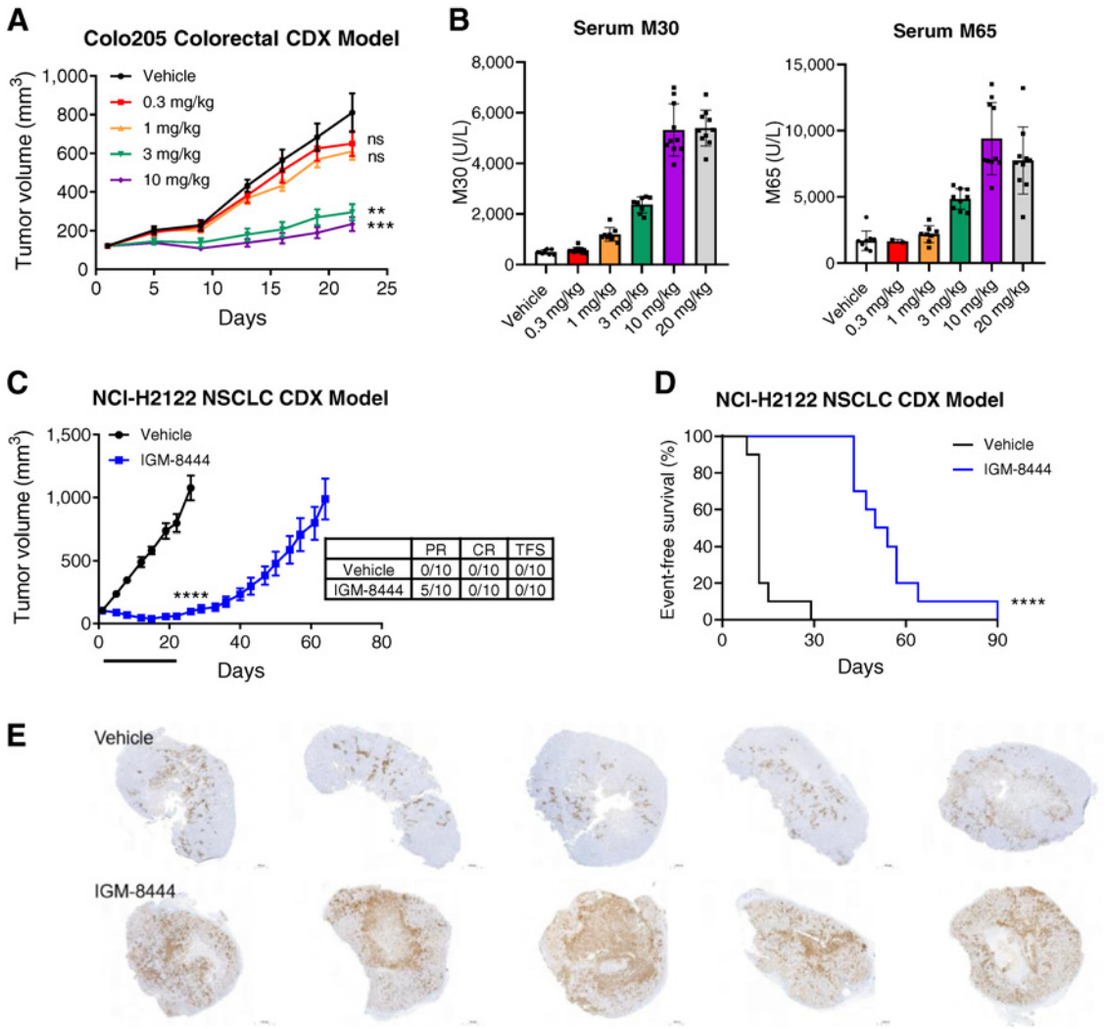


**Figure 4.**

IGM-8444 antitumor efficacy in CDX mouse tumor models. Efficacy and pharmacodynamic biomarkers were evaluated in a Colo205 tumor xenograft model. **A,** Animals were treated with vehicle or 0.3, 1, 3, or 10 mg/kg IGM-8444 i.v. every other day for 11 doses. **B,** A single intravenous dose of IGM-8444 was administered at 0.3, 1, 3, 10, or 20 mg/kg, serum was collected after 24 hours, and M30 and M65 levels were quantitated. **C,** Antitumor efficacy and (**D**) event-free survival in an NCI-H2122 lung model treated with vehicle or 5 mg/kg IGM-8444 i.v. every other day for 11 doses. **E,** NCI-H2122 tumor-bearing mice were dosed once with 5 mg/kg IGM-8444 or vehicle, and after 24 hours tumors were stained for CC3. Shown are representative tumors from 5 mice/group. Tumor volumes represent mean ± SEM, 10 mice/group. **, $P \leq 0.01$; ***, $P \leq 0.001$; ****, $P \leq 0.0001$; ns, not significant.

### IGM-8444 induced complete regression in a gastric PDX tumor model

IGM-8444 *in vivo* efficacy was evaluated in a gastric PDX model, GXF251, established from a 60-year-old male patient with gastric adenocarcinoma. IGM-8444, dosed 5 mg/kg every other day for 7 doses, induced strong and sustained tumor regressions and showed 112% TGI compared with the control group on day 46 ($P \leq 0.0001$; **Fig. 5A**). Eight out of 10 animals in the IGM-8444–treated group exhibited CRs, with the remaining 2 animals showing a PR. At study end (day 99), 7/10 animals were event-free and 6/10 were tumor-free (**Fig. 5B**). Serum analyses 24 hours after IGM-8444 treatment indicated 10- and 6-fold increased M30 and M65, respectively, compared with vehicle (**Fig. 5C**).

IGM-8444 demonstrated dose-dependent efficacy in the GXF251 tumor model (Supplementary Fig. S5A). On day 59, the 0.3, 1, 3, and 10 mg/kg treatment groups showed 30%, 55%, 101% ($P \leq 0.001$), and 99% ($P \leq 0.001$) TGI, respectively, compared with vehicle. On day 100, no animals in the 10 mg/kg dose group had reached study endpoint and 2/7 animals were tumor-free.

IGM-8444 also exhibited dose-dependent efficacy when administered weekly, with 10 mg/kg IGM-8444 maintaining tumor stasis during the dosing period (Supplementary Fig. S5B). On day 28, the 1 and 10 mg/kg treatment groups showed 58% and 102% ($P \leq 0.0001$) TGI, respectively, compared with the control group. Both weekly and every other day IGM-8444 dosing did not cause body weight loss or other toxicities in mice.

Efficacy of IGM-8444 was observed even in large, established tumors. IGM-8444 was dosed 5 mg/kg every other day for 7 doses when MTV reached 100, 300, or 500 $mm^3$ (small, medium, and large tumors). In all cases, IGM-8444 induced significant and comparable levels of tumor regression, measured by absolute and relative tumor volumes (Supplementary Fig. S5C; **Fig. 5D**). On day 32, the small, medium, and large tumors showed 112%, 103%, and 101% TGI, respectively, compared with vehicle ($P \leq 0.001$).

### IGM-8444 enhanced antitumor efficacy in combination with chemotherapy or ABT-199

IGM-8444 was tested in combination with SOC chemotherapy *in vivo*. Irinotecan and 5-FU were evaluated in the Colo205 model because they are widely used in FOLFIRI treatment of patients with colorectal carcinoma. IGM-8444 dosed at 5 mg/kg induced 70%–76% TGI ($P \leq 0.05$) compared with vehicle (**Fig. 6A–C**), consistent with

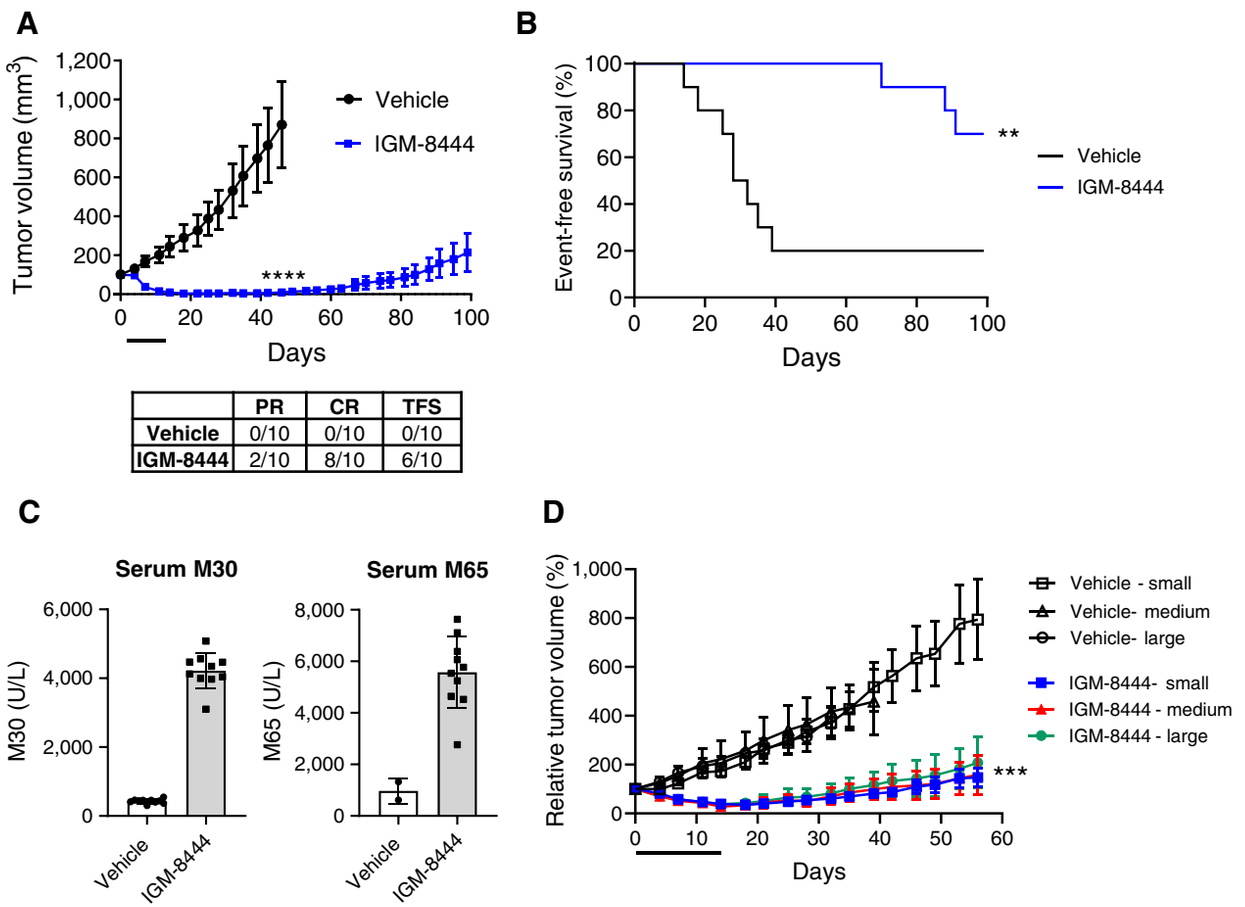


| | PR | CR | TFS |
|---|---|---|---|
| Vehicle | 0/10 | 0/10 | 0/10 |
| IGM-8444 | 2/10 | 8/10 | 6/10 |

**Figure 5.**
IGM-8444 antitumor efficacy in a gastric PDX mouse tumor model. GXF251 tumor-bearing mice were treated with vehicle or 5 mg/kg of IGM-8444 i.v. every other day for 7 doses. **A,** Tumor volumes and (**B**) EFS through day 99 show 6 TFS in the IGM-8444 treated group. **C,** 24 hours after dose, M30 and M65 were measured in serum. **D,** Vehicle or 5 mg/kg IGM-8444 was dosed every other day intravenously for 7 doses when MTV reached approximately 100, 300, or 500 $mm^3$, defined as small, medium, and large tumors, respectively. Tumor volumes represent mean ± SEM, 8–10 mice/group. **, $P \leq 0.01$; ***, $P \leq 0.001$; and ****, $P \leq 0.0001$.

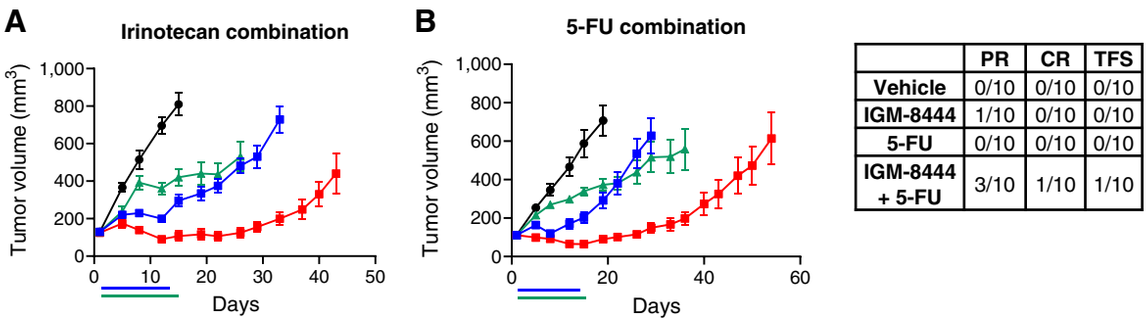


| | PR | CR | TFS |
|---|---|---|---|
| Vehicle | 0/10 | 0/10 | 0/10 |
| IGM-8444 | 1/10 | 0/10 | 0/10 |
| 5-FU | 0/10 | 0/10 | 0/10 |
| IGM-8444 + 5-FU | 3/10 | 1/10 | 1/10 |

| | PR | CR | TFS |
|---|---|---|---|
| Vehicle | 0/10 | 0/10 | 0/10 |
| IGM-8444 | 0/10 | 0/10 | 0/10 |
| Paclitaxel | 7/10 | 3/10 | 2/10 |
| IGM-8444 + Paclitaxel | 0/10 | 10/10 | 8/10 |

| | PR | CR | TFS |
|---|---|---|---|
| Vehicle | 0/10 | 0/10 | 0/10 |
| IGM-8444 | 0/10 | 0/10 | 0/10 |
| ABT-199 | 0/10 | 0/10 | 0/10 |
| IGM-8444 + ABT-199 | 3/10 | 2/10 | 0/10 |

**Figure 6.**

Antitumor efficacy of IGM-8444 in combination with chemotherapeutic and targeted agents. Colo205 tumor-bearing mice were treated with vehicle or 5 mg/kg IGM-8444 i.v. every other day for 7 doses as a single agent and in combination with (**A**) 100 mg/kg irinotecan i.p. weekly for 3 weeks, (**B**) 100 mg/kg 5-FU i.p. weekly for 3 weeks, or (**C**) 25 mg/kg paclitaxel i.v. every other day for 5 doses. **D,** DOHH-2 tumor-bearing mice were treated with vehicle or 5 mg/kg IGM-8444 i.v. every other day for 11 doses, 100 mg/kg ABT-199 p.o. daily for 21 days, or a combination of the IGM-8444 and ABT-199 dosing regimens. Results represent mean ± SEM, 10 mice/group.

previous data (**Fig. 4A**). Irinotecan alone partially reduced tumor volume compared with vehicle (57% TGI, $P > 0.05$), whereas combination of IGM-8444 with irinotecan resulted in tumor stasis during the dosing period (103% TGI, $P \leq 0.0001$) and 2/10 PRs (**Fig. 6A**). Relative to vehicle, combination extended median EFS by 42 days ($P \leq 0.001$; Supplementary Fig. S6A). IGM-8444 and irinotecan combination was significantly more efficacious than irinotecan alone, for both TGI ($P \leq 0.01$) and EFS ($P \leq 0.01$).

5-FU alone partially reduced tumor burden (56% TGI, $P > 0.05$) but also caused toxicity indicated by body weight loss (8.7% ± 6.9% by day 19; **Fig. 6B**). Combination of IGM-8444 with 5-FU significantly enhanced antitumor efficacy compared with vehicle (104% TGI, $P \leq 0.0001$) and 5-FU alone ($P \leq 0.01$) without additional weight loss (5.7% ± 4.2% by day 19). The combination also significantly extended EFS compared with vehicle ($P \leq 0.05$), though not compared with 5-FU alone (Supplementary Fig. S6B). IGM-8444 and 5-FU combined treatment resulted in 3/10 PRs and 1/10 CR that was tumor-free at study end.

Paclitaxel combination with IGM-8444 also exhibited increased activity *in vivo*. Paclitaxel alone induced strong tumor regressions in all 10 animals, with 7 PRs and 3 CRs (**Fig. 6C**). Combination with IGM-8444 increased the CR rate from 30% to 100% and improved EFS (Supplementary Fig. S6C). When the study was terminated on day 100, 2/10 animals in the paclitaxel-treated group had no visible tumors, whereas 8/10 animals in the combined treatment arm were tumor-free.

Finally, IGM-8444 was evaluated in combination with ABT-199, a BCL-2 inhibitor targeting the intrinsic apoptotic pathway, in the NHL model DOHH-2. Over 21 days, IGM-8444 was administered every other day and ABT-199 was given daily. By day 16, both IGM-8444 and ABT-199 showed modest single-agent efficacy compared with vehicle with 45% and 60% TGI ($P \leq 0.01$), respectively (**Fig. 6D**). Combination of IGM-8444 with ABT-199 induced 102% TGI compared with control ($P \leq 0.0001$), with 3/10 PRs and 2/10 CRs. Combined treatment significantly extended median EFS compared with vehicle ($P \leq 0.001$) or ABT-199 alone ($P \leq 0.001$; Supplementary Fig. S6D). In summary, these results suggest that antitumor efficacy may be significantly enhanced by combining IGM-8444 with SOC chemotherapy or targeted agents such as BCL-2 inhibitors.

## Discussion

DR5 has been a long sought-after cancer target; however, agonistic DR5 IgG antibodies have failed clinically likely due to insufficient crosslinking by FcγR-expressing cells necessary to

induce apoptosis (1). Currently, only one anti-DR5 IgG antibody remains under clinical evaluation, DS-8273a in combination with nivolumab (anti–PD-1; ref. 32). A new generation of DR5 superagonists capable of enhanced receptor multimerization is now under investigation. Clinical trials of tetravalent nanobody TAS266 were terminated due to acute hepatic toxicity associated with anti-drug antibodies (30, 33). RG7386, a tetravalent bispecific antibody targeting DR5 and fibroblast activation protein (FAP) expressed on tumor fibroblasts, was developed with the goal of localizing antibody to tumor and crosslinking DR5 via FAP binding (34). Antitumor activity was observed in 1/32 patients, although it is unclear whether FAP binding mediated sufficient DR5 clustering to induce tumor cytotoxicity (35). Current clinical trials are evaluating four multivalent DR5-targeting molecules: ABBV-621, a hexavalent TRAIL–Fc fusion protein (36, 37), GEN1029, a hexamerizing IgG (38, 39), INBRX-109, a tetravalent single-domain antibody, and BI 905711, a tetravalent bispecific antibody targeting DR5 and cadherin 17 (CDH17; ref. 31). Some of these agonists have shown signs of clinical efficacy, but liver toxicity has also been reported (36).

IgM antibodies are the first antibodies to appear in response to a foreign antigen. Natural IgM antibodies are characterized by high-avidity, low-affinity binding to repetitive carbohydrate and lipid antigens (40). Because of its multivalent structure, IgM effectively binds complement component 1q (C1q) and eliminates pathogens through complement-dependent cytotoxicity. Consequently, IgM antibodies have been investigated in infectious disease, oncology, and autoimmune disease clinical trials though no therapeutic IgM antibodies have been FDA approved (reviewed in ref. 41). A potential reason is that most clinically evaluated IgM antibodies were originally isolated from patients and, therefore, had strong avidity but low affinity and specificity.

Here, we demonstrate the preclinical efficacy of IGM-8444, an engineered DR5 IgM agonistic antibody with high avidity, affinity, and specificity capable of clustering DR5 to induce cancer cell cytotoxicity. IGM-8444 exhibited stronger binding and induced more rapid and potent tumor cell apoptosis compared with an IgG with the same binding domain. The faster kinetics of caspase induction are consistent with crosslinking-independent receptor clustering by IgM, as has been observed with other multivalent agonists (30, 38, 42). IGM-8444 demonstrated low picomolar potency across multiple solid and hematologic cancer cell lines, induced tumor regressions or stasis in mouse xenograft tumor models and caused dose-dependent increases in apoptotic biomarkers. Notably, IGM-8444 induced tumor regressions in large established tumors.

One theoretical concern is that the large molecular weight of IgM antibodies may hinder tumor penetration compared with IgGs. However, on the basis of the substantial tumor regressions observed in large established gastric PDX tumors upon IGM-8444 treatment, the increased size and molecular radius of an IgM does not appear to prevent tumor penetration and these results are encouraging for treatment of advanced carcinomas. The IgM format structurally differentiates IGM-8444 from other multivalent DR5 agonists and enables it to more efficiently multimerize DR5 to overcome limitations of IgG agonists, which require FcγR engagement for crosslinking. The multivalency of IGM-8444 may also provide benefit over IgG agonists in terms of retaining activity in the presence of soluble DR5 (sDR5), which can act as a sink and limit clinical efficacy.

Historically, the predominant safety concern for DR5 agonists has been liver toxicity. A key feature of IGM-8444 is its lack of cytotoxicity on primary human hepatocytes *in vitro*, either as a single agent or in combination with several SOC agents. The results of our combination studies are consistent with previous reports that TRAIL may be combined with several chemotherapies without causing hepatotoxicity (43). IGM-8444 was also safe in cynomolgus monkey studies with no evidence of hepatotoxicity. Collectively, the favorable preclinical safety profile of IGM-8444 may enable combination opportunities that would otherwise be unviable.

Some studies have reported no association between DR5 expression and sensitivity to DR5 agonists, whereas others have observed a correlation (8, 9, 31, 34, 37, 44), In a screen of 190 cancer cell lines, IGM-8444 response was associated with higher DR5 expression levels. Incomplete cytotoxicity was seen in some cell lines even at saturating concentrations of IGM-8444, suggesting tumor heterogeneity, DR5 downregulation, or upregulation of apoptotic resistance mechanisms. Regulators in the extrinsic and intrinsic (mitochondrial) apoptotic pathways such as CASP8, BID, and cFLIP have been reported to contribute to anti-DR5 sensitivity (45), and our ongoing studies aim to understand the genes and pathways that influence IGM-8444 sensitivity. Partially sensitive models are ideal candidates for combination treatment, and we have demonstrated enhanced antitumor efficacy in Colo205 models treated with IGM-8444 in combination with irinotecan, 5-FU, or paclitaxel. The combinatorial effects may be due to mRNA upregulation of DR5, upregulation of pro-apoptotic regulators such as BAX and CASP9, or downregulation of anti-apoptotic regulators such as cFLIP and Survivin (46–49). Moreover, combination of IGM-8444 with BCL-2 inhibitor ABT-199 in an NHL model resulted in tumor regressions and improved efficacy compared with either single agent. BCL-2 inhibitors are among several therapeutic approaches currently in development targeting the intrinsic apoptotic pathway, and thus far ABT-199 has been approved in AML, CLL, and SLL and is under investigation in NHL and other hematologic malignancies (50). Our results provide a strong rationale for simultaneously targeting the extrinsic and intrinsic apoptotic pathways to overcome apoptotic resistance mechanisms and improve efficacy.

In summary, we have generated a novel engineered multivalent agonistic DR5 IgM antibody IGM-8444, which effectively clusters DR5 to potently induce tumor cell apoptosis *in vitro* and *in vivo* with minimal to no *in vitro* hepatotoxicity. IGM-8444 induced tumor regressions in xenograft models, including large established tumors, and potently combined with chemotherapy or a BCL-2 inhibitor. These data support clinical development of IGM-8444 with potential to treat both solid and hematologic malignancies and a Phase 1 study is currently ongoing (NCT04553692). Recombinant, high-affinity, high-avidity IgM antibodies are a promising therapeutic modality with potential clinical advantages over traditional IgG antibodies.

## Authors' Disclosures

B.T. Wang reports employment with and is a stockholder of IGM Biosciences Inc. outside the submitted work; as well as being an inventor on a patent entitled "Tumor necrosis factor (TNF) Superfamily Receptor-Binding Molecules and Uses Thereof," patents and pending applications entitled "Multimeric Death Domain-Containing Receptor-5 (DR5) Antibodies and Method Thereof to Treat Cancer," and pending patent applications entitled "Use of a Multimeric Anti-DR5-Binding Molecule in Combination with a Chemotherapeutic Agent for Treating Cancer," which are assigned to IGM Biosciences Inc. T. Kothambawala reports employment with and is a stockholder of IGM Biosciences Inc. outside the submitted work. L. Wang reports

employment with and is a stockholder of IGM Biosciences Inc. outside the submitted work. T.J. Matthew reports employment with and is a stockholder of IGM Biosciences Inc. outside the submitted work. S.E. Calhoun reports employment with and is a stockholder of IGM Biosciences Inc. outside the submitted work. A.K. Saini reports employment with and is a stockholder of IGM Biosciences Inc. outside the submitted work. M.F. Kotturi reports employment with and is a stockholder of IGM Biosciences Inc. outside the submitted work. G. Hernandez reports employment with and is a stockholder of IGM Biosciences Inc. outside the submitted work. E.W. Humke reports employment with and is a stockholder of IGM Biosciences Inc. outside the submitted work. M.S. Peterson reports employment with and is a stockholder of IGM Biosciences Inc. outside the submitted work. A.M. Sinclair reports employment with and is a stockholder of IGM Biosciences Inc. outside the submitted work. B.A. Keyt reports employment with and is a stockholder of IGM Biosciences Inc. outside the submitted work; as well as being an inventor on a patent entitled "Tumor necrosis factor (TNF) Superfamily Receptor-Binding Molecules and Uses Thereof," patents and pending applications entitled "Multimeric Death Domain-Containing Receptor-5 (DR5) Antibodies and Method Thereof to Treat Cancer," and pending patent applications entitled "Use of a Multimeric Anti-DR5-Binding Molecule in Combination with a Chemotherapeutic Agent for Treating Cancer," which are assigned to IGM Biosciences Inc.

## Authors' Contributions

**B.T. Wang:** Conceptualization, formal analysis, supervision, validation, investigation, visualization, methodology, writing–original draft, project administration, writing–review and editing. **T. Kothambawala:** Validation, investigation, visualization, methodology, writing–original draft. **L. Wang:** Validation, investigation, visualization, methodology, writing–original draft. **T.J. Matthew:** Data curation, software, formal analysis, validation, visualization, methodology, writing–original draft. **S.E. Calhoun:** Formal analysis, validation, investigation, visualization, writing–original draft. **A.K. Saini:** Resources. **M.F. Kotturi:** Investigation, writing–review and editing. **G. Hernandez:** Writing–review and editing. **E.W. Humke:** Writing–review and editing. **M.S. Peterson:** Resources. **A.M. Sinclair:** Conceptualization, supervision, validation, visualization, methodology, writing–original draft, project administration, writing–review and editing. **B.A. Keyt:** Conceptualization, supervision, funding acquisition, writing–review and editing.

## Acknowledgments

The authors thank Steve Carroll, Ramesh Baliga, and Catherine Lucas for helpful discussions, Poonam Yakkundi for help with efficacy studies, and Devinder Ubhi and Palak Chudasama for performing analytical assays. We also thank Paul Schnier for avidity analyses, Yuan Cao and Maya Leabman for pharmacokinetic and cynomolgus monkey studies, and Bing Shan, Hai Lu, and Erick Morales for antibody purification. Finally, we thank the teams at CRL for performing efficacy studies, Crown Bioscience for performing cell line screening and chemotherapy combination assays, Invicro for performing IHC, Biosensor Tools for SPR studies, Integral Molecular for epitope mapping studies, and Cellecta for generating DR5 KO cells. This work was supported by IGM Biosciences Inc.

The costs of publication of this article were defrayed in part by the payment of page charges. This article must therefore be hereby marked *advertisement* in accordance with 18 U.S.C. Section 1734 solely to indicate this fact.

Received December 31, 2020; revised July 7, 2021; accepted September 15, 2021; published first October 28, 2021.

## References

1. Holland PM. Death receptor agonist therapies for cancer, which is the right TRAIL? Cytokine Growth Factor Rev 2014;25:185–93.
2. Sheridan JP, Marsters SA, Pitti RM, Gurney A, Skubatch M, Baldwin D, et al. Control of TRAIL-induced apoptosis by a family of signaling and decoy receptors. Science 1997;277:818–21.
3. Ichikawa K, Liu W, Zhao L, Wang Z, Liu D, Ohtsuka T, et al. Tumoricidal activity of a novel anti-human DR5 monoclonal antibody without hepatocyte cytotoxicity. Nat Med 2001;7:954–60.
4. Ashkenazi A, Holland P, Eckhardt SG. Ligand-based targeting of apoptosis in cancer: the potential of recombinant human apoptosis ligand 2/Tumor necrosis factor-related apoptosis-inducing ligand (rhApo2L/TRAIL). J Clin Oncol 2008; 26:3621–30.
5. Kaplan-Lefko PJ, Graves JD, Zoog SJ, Pan Y, Wall J, Branstetter DG, et al. Conatumumab, a fully human agonist antibody to death receptor 5, induces apoptosis via caspase activation in multiple tumor types. Cancer Biol Ther 2010; 9:618–31.
6. Adams C, Totpal K, Lawrence D, Marsters S, Pitti R, Yee S, et al. Structural and functional analysis of the interaction between the agonistic monoclonal antibody Apomab and the proapoptotic receptor DR5. Cell Death Differ 2008;15:751–61.
7. Marini P, Denzinger S, Schiller D, Kauder S, Welz S, Humphreys R, et al. Combined treatment of colorectal tumours with agonistic TRAIL receptor antibodies HGS-ETR1 and HGS-ETR2 and radiotherapy: enhanced effects *in vitro* and dose-dependent growth delay *in vivo*. Oncogene 2006;25:5145–54.
8. Yada A, Yazawa M, Ishida S, Yoshida H, Ichikawa K, Kurakata S, et al. A novel humanized anti-human death receptor 5 antibody CS-1008 induces apoptosis in tumor cells without toxicity in hepatocytes. Ann Oncol 2008;19:1060–7.
9. Li J, Knee DA, Wang Y, Zhang Q, Johnson JA, Cheng J, et al. LBY135, a novel anti-DR5 agonistic antibody induces tumor cell–specific cytotoxic activity in human colon tumor cell lines and xenografts. Drug Dev Res 2008;69:69–82.
10. Ashkenazi A, Pai RC, Fong S, Leung S, Lawrence DA, Marsters SA, et al. Safety and antitumor activity of recombinant soluble Apo2 ligand. J Clin Invest 1999; 104:155–62.
11. Kimotsuki T, Tanaka K, Sugiura T, Koyama K, Nakamura T, Kamimura Y, et al. Thirteen-week intravenous toxicity study of a novel humanized anti-human death receptor 5 monoclonal antibody, CS-1008, in cynomolgus monkeys. J Toxicol Pathol 2010;23:11–7.
12. Chen W, Qiu L, Hou J, Zhao Y, Pan L, Yang S, et al. Recombinant circularly permuted TRAIL (CPT) for the treatment of relapsed or refractory multiple myeloma: an open-label, multicenter phase II clinical trial [abstract]. Blood 2012; 120:78.
13. Camidge DR, Herbst RS, Gordon MS, Eckhardt SG, Kurzrock R, Durbin B, et al. A phase I safety and pharmacokinetic study of the death receptor 5 agonistic antibody PRO95780 in patients with advanced malignancies. Clin Cancer Res 2010;16:1256–63.
14. Lemke J, von Karstedt S, Zinngrebe J, Walczak H. Getting TRAIL back on track for cancer therapy. Cell Death Differ 2014;21:1350–64.
15. Herbst RS, Eckhardt SG, Kurzrock R, Ebbinghaus S, O'Dwyer PJ, Gordon MS, et al. Phase I dose-escalation study of recombinant human Apo2L/TRAIL, a dual proapoptotic receptor agonist, in patients with advanced cancer. J Clin Oncol 2010;28:2839–46.
16. Pan L, Fu TM, Zhao W, Zhao L, Chen W, Qiu C, et al. Higher-order clustering of the transmembrane anchor of DR5 drives signaling. Cell 2019; 176:1477–89.
17. Wang B, Kothambawala T, Wang L, Saini A, Baliga R, Sinclair A, et al. Multimeric IgM antibodies targeting DR5 are potent and rapid inducers of tumor cell apoptosis and cell death *in vitro* and *in vivo* [abstract]. In: Proceedings of American Association for Cancer Research Conference; 2019 Mar 29–Apr 3; Atlanta, GA: AACR; 2019. Abstract nr 3050.
18. Wang B, Kothambawala T, Hinton P, Ng D, Saini A, Baliga R, et al. Multimeric anti-DR5 IgM antibody displays potent cytotoxicity *in vitro* and promotes tumor regression *in vivo* [abstract]. In: Proceedings of American Association for Cancer Research Conference; 2017 April 1–5; Washington, DC: AACR; 2017. Abstract nr 1702.
19. Piao X, Ozawa T, Hamana H, Shitaoka K, Jin A, Kishi H, et al. TRAIL-receptor 1 IgM antibodies strongly induce apoptosis in human cancer cells *in vitro* and *in vivo*. Oncoimmunology 2016;5:e1131380.
20. Guo L, Sun X, Hao Z, Huang J, Han X, You Y, et al. Identification of novel epitopes with agonistic activity for the development of tumor immunotherapy targeting TRAIL-R1. J Cancer 2017;8:2542–53.
21. Chen Y, Paluch M, Zorn JA, Rajan S, Leonard B, Estevez A, et al. Targeted IgMs agonize ocular targets with extended vitreal exposure. mAbs 2020;12: e1818436.
22. Gagnon P. Monoclonal antibody purification with hydroxyapatite. N Biotechnol 2009;25:287–93.
23. Hafner M, Niepel M, Chung M, Sorger PK. Growth rate inhibition metrics correct for confounders in measuring sensitivity to cancer drugs. Nat Methods 2016;13:521–7.
24. Ianevski A, Giri AK, Aittokallio T. SynergyFinder 2.0: visual analytics of multi-drug combination synergies. Nucleic Acids Res 2020;48:W488–93.
25. Bliss CI. The toxicity of poisons applied jointly. Ann App Biol 1939;26:585–615.

26. Chaudhary PM, Eby M, Jasmin A, Bookwalter A, Murray J, Hood L. Death receptor 5, a new member of the TNFR family, and DR4 induce FADD-dependent apoptosis and activate the NF-kappaB pathway. Immunity 1997;7: 821–30.
27. Schneider P, Bodmer JL, Thome M, Hofmann K, Holler N, Tschopp J. Characterization of two receptors for TRAIL. FEBS Lett 1997;416:329–34.
28. Marsters SA, Sheridan JP, Pitti RM, Huang A, Skubatch M, Baldwin D, et al. A novel receptor for Apo2L/TRAIL contains a truncated death domain. Curr Biol 1997;7:1003–6.
29. Wang BT, Kothambawala T, Hart KC, Chen X, Desbois M, Calhoun SE, et al. Mechanistic evaluation of anti-DR5 IgM antibody IGM-8444 with potent tumor cytotoxicity, without in vitro hepatotoxicity [abstract]. In: Proceedings of the American Association for Cancer Research Annual Meeting 2021; 2021 Apr 10–15 and May 17–21. Philadelphia (PA): AACR; Cancer Res 2021;81(13_Suppl): Abstract nr 52.
30. Huet HA, Growney JD, Johnson JA, Li J, Bilic S, Ostrom L, et al. Multivalent nanobodies targeting death receptor 5 elicit superior tumor cell killing through efficient caspase induction. MAbs 2014;6:1560–70.
31. García-Martínez JM, Wang S, Weishaeupl C, Wernitznig A, Chetta P, Pinto C, et al. Selective tumor cell apoptosis and tumor regression in CDH17-positive colorectal cancer models using BI 905711, a novel liver-sparing TRAILR2 agonist. Mol Cancer Ther 2021;20:96–108.
32. Dominguez GA, Condamine T, Mony S, Hashimoto A, Wang F, Liu Q, et al. Selective targeting of myeloid-derived suppressor cells in cancer patients using DS-8273a, an agonistic TRAIL-R2 antibody. Clin Cancer Res 2017;23: 2942–50.
33. Papadopoulos KP, Isaacs R, Bilic S, Kentsch K, Huet HA, Hofmann M, et al. Unexpected hepatotoxicity in a phase I study of TAS266, a novel tetravalent agonistic Nanobody targeting the DR5 receptor. Cancer Chemother Pharmacol 2015;75:887–95.
34. Brünker P, Wartha K, Friess T, Grau-Richards S, Waldhauer I, Koller CF, et al. RG7386, a novel tetravalent FAP-DR5 antibody, effectively triggers FAP-dependent, avidity-driven DR5 hyperclustering and tumor cell apoptosis. Mol Cancer Ther 2016;15:946–57.
35. Bendell J, Blay J, Cassier P, Bauer T, Terret C, Mueller C, et al. Phase 1 trial of RO6874813, a novel bispecific FAP-DR5 antibody, in patients with solid tumors [abstract]. In: Proceedings of the AACR-NCI-EORTC International Conference: molecular targets and cancer therapeutics; 2017 Oct 26–30; Philadelphia, PA: AACR; 2018. Abstract nr A092.
36. Ratain MJ, Doi T, De Jonge MJ, LoRusso P, Dunbar M, Chiney M, et al. Phase 1, first-in-human study of TRAIL receptor agonist fusion protein ABBV-621 [abstract]. Journal of Clinical Oncology 2019;37:15_suppl, 3013–3013.
37. Phillips DC, Buchanan FG, Cheng D, Solomon LR, Xiao Y, Xue J, et al. Hexavalent TRAIL fusion protein eftozanermin alfa optimally clusters apoptosis-inducing TRAIL receptors to induce on-target antitumor activity in solid tumors. Cancer Res 2021;81:3402–14.
38. van der Horst HJ, Overdijk MB, Breij ECW, Chamuleau M, Lokhorst HM, Mutis T. Potent ex vivo anti-tumor activity in relapsed refractory multiple myeloma using novel DR5-specific antibodies with enhanced capacity to form hexamers upon target binding [abstract]. In: Proceedings of the American Society of Hematology Conference; 2017 Dec 9–12; Atlanta, GA. Washington, DC: ASH; 2017. Abstract nr 1835.
39. Overdijk MB, Strumane K, Beurskens FJ, Ortiz Buijsse A, Vermot-Desroches C, Vuillermoz BS, et al. Dual epitope targeting and enhanced hexamerization by DR5 antibodies as a novel approach to induce potent antitumor activity through DR5 agonism. Mol Cancer Ther 2020;19:2126–38.
40. Boes M. Role of natural and immune IgM antibodies in immune responses. Mol Immunol 2000;37:1141–9.
41. Keyt BA, Baliga R, Sinclair AM, Carroll SF, Peterson MS. Structure, function, and therapeutic use of IgM antibodies. Antibodies 2020;9:53.
42. Gieffers C, Kluge M, Merz C, Sykora J, Thiemann M, Schaal R, et al. APG350 induces superior clustering of TRAIL receptors and shows therapeutic antitumor efficacy independent of cross-linking via Fcγ receptors. Mol Cancer Ther 2013; 12:2735–47.
43. Koschny R, Walczak H, Ganten TM. The promise of TRAIL—potential and risks of a novel anticancer therapy. J Mol Med 2007;85:923–35.
44. Graves JD, Kordich JJ, Huang TH, Piasecki J, Bush TL, Sullivan T, et al. Apo2L/TRAIL and the death receptor 5 agonist antibody AMG 655 cooperate to promote receptor clustering and antitumor activity. Cancer Cell 2014;26:177–89.
45. Reddy A, Growney JD, Wilson NS, Emery CM, Johnson JA, Ward R, et al. Gene expression ratios lead to accurate and translatable predictors of DR5 agonism across multiple tumor lineages. PLoS One 2015;10:e0138486.
46. Zhu H, Zhao F, Yu S, He J, Deng L, Yi C, et al. The synergistic effects of low-dose irinotecan and TRAIL on TRAIL-resistant HT-29 colon carcinoma *in vitro* and *in vivo*. Int J Mol Med 2012;30:1087–94.
47. Galligan L, Longley DB, McEwan M, Wilson TR, McLaughlin K, Johnston PG. Chemotherapy and TRAIL-mediated colon cancer cell death: the roles of p53, TRAIL receptors, and c-FLIP. Mol Cancer Ther 2005;4:2026–36.
48. Yang L, Wang Y, Zheng H, Zhang D, Wu X, Sun G, et al. Low-dose 5-fluorouracil sensitizes HepG2 cells to TRAIL through TRAIL receptor DR5 and survivin-dependent mechanisms. J Chemother 2017;29:179–88.
49. Gong J, Yang D, Kohanim S, Humphreys R, Broemeling L, Kurzrock R. Novel *in vivo* imaging shows upregulation of death receptors by paclitaxel and correlates with enhanced antitumor effects of receptor agonist antibodies. Mol Cancer Ther 2006;5:2991–3000.
50. Carneiro BA, El-Deiry WS. Targeting apoptosis in cancer therapy. Nat Rev Clin Oncol 2020;17:395–417.